Direct measurement of carbon dioxide removal due to enhanced weathering

Ella Milliken[1], Alex Woodley[2], Noah Planavsky[1,3]

1. Earth & Planetary Sciences, Yale University, New Haven, CT, 06520
2. Department of Crop and Soil Sciences, North Carolina State University, Raleigh, NC, 27695
3. Yale Center For Natural Carbon Capture, Yale University, New Haven, CT, 06520

Corresponding Author: Ella Milliken, ella.milliken@yale.edu

Abstract

Enhanced weathering (EW) is a durable carbon removal strategy with clear pathways to produce significant global supply on a decadal scale. Despite increasing interest and investment in this process, there have been limited direct, continuous observations of weathering rates. In this study, we monitor a basalt-applied soybean plot in Southeast Virginia using continuous in-soil CO_2 monitors. We provide clear evidence of CO_2 flux reduction within the soil profile, equating to 1.04 t $ha^{-1}yr^{-1}$. This removal is most substantial in the active growing season and following significant rain pulses. This work supports that direct and continuous gas-phase measurements will play an important role in advancing our understanding of the timescale of enhanced weathering rates, and demonstrating enhanced weathering to be a rigorous, scalable method of durable carbon removal.

Keywords: enhanced weathering, carbon dioxide removal, in-soil CO_2, gas-phase MRV, time-lag

Synopsis: There has been a lack of direct evidence of CO_2 drawdown from enhanced weathering. This study demonstrates that basalt addition in agricultural fields leads to soil CO_2 profile reductions.

Introduction

There is a significant gap between current global emissions and Paris Agreement goals to remain below 2°C of warming[1]. Carbon dioxide removal (CDR) has become incorporated in the projected greenhouse gas budgets of many nations for the coming century[2,3]. There has been accompanying global investment in durable CDR, with many countries supporting demonstration projects and developing related policy[2,4]. Despite notable advances in deployment within the past decade, there is still a massive discrepancy between global estimates of durable CDR demand and supply[2,5–7].

Enhanced weathering (EW) is a geochemical CDR strategy with a pathway to hit gigaton-scale removal this century, with recent estimates projecting up to 0.5 $GtCO_2$ yr^{-1} of removal by 2070[8]. EW builds on our understanding of natural silicate weathering, a climatic feedback on geologic timescales. In EW deployments, crushed, reactive silicate rock is applied to terrestrial environments to foster rapid weathering rates, ultimately increasing the alkalinity of the system by releasing major base cations[9]. The resulting pH and micronutrient increase from this reaction has been of particular interest for terrestrial agricultural systems, where low fertility is a persistent issue which will only be exacerbated by climate change[10–13].

Current best-practice EW field quantification methods rely on aqueous and solid phase cation measurements to quantify CDR rates in EW deployments[14–16]. Aqueous phase measurements, such as porewaters or catchment samples, can be measured directly for total alkalinity (TA)[6,9–11]. However, generating continuous accurate data from aqueous measurements is not currently possible, and traditional methods are labor intensive[15]. Further, watershed signals can be highly dilute in large catchments, and may require geochemical tracers to provide evidence of weathering[17]. Soil-based cation mass balance approaches will intrinsically give a maximum estimation of CDR within the system, and there may be significant time delays between soil signals and decreased CO_2 fluxes due to cation sorption within the soil column[18].

CO_2 gas flux measurement is an obvious complement to aqueous and solid phase methods of tracking weathering rates. This method provides the most direct measure of field-scale carbon removal rates. Previously, EW gas measurements have focused on using aboveground flux chambers and eddy covariance towers to approximate weathering. These methods have high signal-to-noise ratios due to diurnal vegetation CO_2 pulses and high surface heterogeneity, making it difficult to produce a substantial signal[19–22]. The use of in-soil CO_2 sensors is a well-established technique for understanding changing soil carbon dynamics[23–25]. However, long-term monitoring of in-soil CO_2 has yet to be studied in an EW system.

Here, we provide direct, gas-phase evidence of CO_2 removal within the soil profile during weathering, using a plot-level experiment over a half-year of monitoring in Southern Virginia, USA. We use a dataset of continually logged soil CO_2 concentration ($[CO_2]$), volumetric water content (θ), temperature, and pressure to give a conservative estimate of immediate CO_2 removal due to enhanced weathering.

Methods

Site Description

The research site is located on a no-till corn-wheat-soy agricultural farm in Clarksville, VA, in the Piedmont region of Southside Virginia. The soil across the study region is a fine, mixed, subactive, thermic, oxyaquatic hapludult, with a parent material of alluvial capped felsic granite. The Ap horizon continues to 22cm, followed by an E horizon to 40 cm, and various B horizons continuing to 130+ cm (SI Fig.1). Soils are homogenous across the study region, with 0-2% slope over the area. For the study season, winter wheat was harvested in early June and soybeans planted in late June. A Farmblox weather station providing temperature and atmospheric pressure data was installed on-site.

Following the planting of Pioneer conventional soybeans and herbicide application in June 2024, a 50' x 108' region with homogenous soils and even prior-season growth was removed from normal practices to use for the gas monitoring array, 20' from a service road. Within the plot, three 28'x36' blocks with 6 ft alleys between them were demarcated, with each block holding sixteen 7'x9' plots. Within each block, 8 plots were randomly selected for basalt application, with a dry application rate of 44.8 t ha^{-1}. No additional fertilizer or amendments were applied to the field within the measurement period. Soybeans were harvested by hand on October 12, 2024, and rye cover crop was immediately applied.

Feedstock Analysis

Applied basalt ($Al_{0.41}Fe_{0.11}(Mg_{.16}Ca_{.14})Si_{1.17}O_2$ based on a total digest of the feedstock) was sourced from Roxboro, North Carolina, with a BET SSA of 5.37 ± 1.2 m^2/g, and p80 = 89.92μm. The BET SSA was given from a 3-point N_2 absorption by Particle

Technology Labs and the PSD was derived from Microtrac Sync by averaging diffraction and dynamic image analysis. The basalt has a TIC content of 0.00196 ± 0.0031 % and was analyzed using an Eltra CS-580A Analyzer.

Soil Analysis

For each individual plot, 15 0-10cm cores were taken and aggregated. Soil samples were collected in June 2024 prior to spreading, then again in October 2024 following soybean harvest. Bulk density samples were collected in December 2024 for each block, with 2 cores being collected for each block every 5 cm, then all values being averaged to give a 0-10 value for each block. All soil samples were analyzed for organic matter (% LOI at 600^{o}C), CEC (Mehlich-3 extraction), pH (DI water), and buffer pH (Mehlich-3 extraction).

Soil Profile Monitoring

Prior to application, 2 control and 2 basalt plots on each block, totaling 6 total control plots and 6 total basalt plots, were selected for in-soil CO_2 installation. Within these blocks, a 4” hole was augured to 15 in. At 10 cm, a Vaisala GMP343, fitted with a horizontal diffusion adapter, was installed pointing north within the soil profile. The probes measure up to 2% CO_2 with ± 2% error. Probes were connected to Farmblox auto-loggers, which recorded raw [CO_2], filtered [CO_2], temperature, and error status every 30s. Auto-logging Farmblox soil moisture/temperature/electrical conductivity probes were installed at 10 cm, measuring properties every 3.5 minutes. CO_2 concentration at all points at 10 cm was recorded from September 2024-February 2025.

Analysis

Soil CO_2 profiles are dynamic on a daily to weekly timescale. However, in short time intervals, the system can be assumed to behave like a steady state system, with macro-scale state shifts, such as erosion, soil production, litter production, porosity, atmospheric CO_2, being considered negligible changes, and micro-scale shifts, such as diurnal CO_2 production, barometric pressure, temperature, θ, considered as temporal shifts that can be incorporated into the flux estimation itself. Within this framework, the profile is assumed to be steady within a fixed depth and time interval. The use of the gradient method for a steady state system has been shown to have good agreement in estimating soil CO_2 flux with continuous monitoring[24].

The CO_2 flux within the soil profile can be solved using Fick's first law:

$$F(x) = -D_s \frac{dC}{dx}$$

With D_s being given by[25–27]:

$$D_s = \frac{\epsilon^{2.5}}{\sqrt{\theta}} D_o$$

$$\phi = 1 - \frac{\rho_s}{\rho_r} = \epsilon + \theta$$

$$D_o = 0.00001381 \cdot \left(\frac{T}{273.15}\right)^{1.81} \cdot \left(\frac{1000}{P}\right)$$

With ϵ = air-filled porosity (cm^3/cm^3), ϕ = total soil porosity (cm^3/cm^3) ρ_s = soil bulk density (g/cm^3), ρ_r = particle density (2.65 g/cm^3), θ = measured volumetric water content (%), T = air temperature (K), and P = air pressure (Pa).

$F_{0\text{-}10}$ (μmol m^{-2} s^{-1}) is approximated using comparisons of atmospheric CO_2 (421 ppm) and averaged soil [CO_2], T, and θ over 15-minute intervals. Values with [CO_2] >30000 ppm, θ > 40%, $F_{0\text{-}10}$ > 40 μmol m^{-2} s^{-1} or a $n \leq 2$ for control and treatment were removed. Significance was determined using a Mann-Whitney test using all replicate measurements binned in 2-hour intervals between control and treatment blocks. There was a data outage from 09-26-2024 to 10-09-2024 due to a hurricane. This data was estimated by fitting an exponential curve to both control and basalt datasets, with the fit data beginning at 9-15-2024. Modeled data from these curves ($R^2_{control}$ = 0.89, R^2_{basalt}= 0.80) was then generated for the time of interest and used to calculate the cumulative flux. The remaining missing values (all with <12 hours of measurement outage) were interpolated linearly. The full dataset was then integrated to give cumulative values. Error is expressed as SEM.

Cation export efficiency

Enhanced weathering will only lead to immediate decrease in CO_2 fluxes when the weathering products are exported below the diffusional active zone of soils. Cations moving onto sorption sites in the upper soil column temporarily reverse the weathering reaction[16]. We generate the efficiency of instantaneous (within a season) weathering product export by comparing the shift in sorbed cations relative to the CO_2 sensor-based flux estimate. Specifically, we translate the change in sorbed cation concentration between spreading (June 20) and resampling (October 20) for basalt and control treatments to a CO_2 flux estimate. For a yearly rate, this value was divided by the fraction of year between sampling events. This does not consider cations sorbed outside of the sampled interval—making it a minimum estimate of the total cation addition into the system. Error is expressed as SEM.

Results and Discussion

Basalt dissolution is indicated in the solid phase through significant increases in pH ($p<0.0001$) and base saturation ($p=0.0007$) from June 2024-October 2024. There was no significant change in organic matter (Fig. 1). The basalt base saturation (%) increased by 10.08 ± 5.6 %, while control increased by 3.37 ± 7.04 %, equating to a minimum weathering rate of 0.44 ± 0.04 $tCO_2\ ha^{-1}$, or 1.34 $tCO_2\ ha^{-1}yr^{-1}$ ± 0.13 $tCO_2\ ha^{-1}yr^{-1}$. This base saturation estimate is conservative; it does not consider cations transported past 10 cm.

There is no significant difference in θ between treatments, but θ did vary over time, directly controlled by precipitation events within the region (Fig. 2a). The CO_2 flux was overall most prominent in the growing season (08/2024-11/2024), with rates staying relatively consistent following cover cropping (11/2024) (Fig. 2b). The flux difference at the beginning of the year is the most prominent, with the maximal difference in flux equating to -1.23 μmol $m^{-2}\ s^{-1}$, and an average decrease of -0.07 μmol $m^{-2}\ s^{-1}$ (Fig. 2b, 2c).

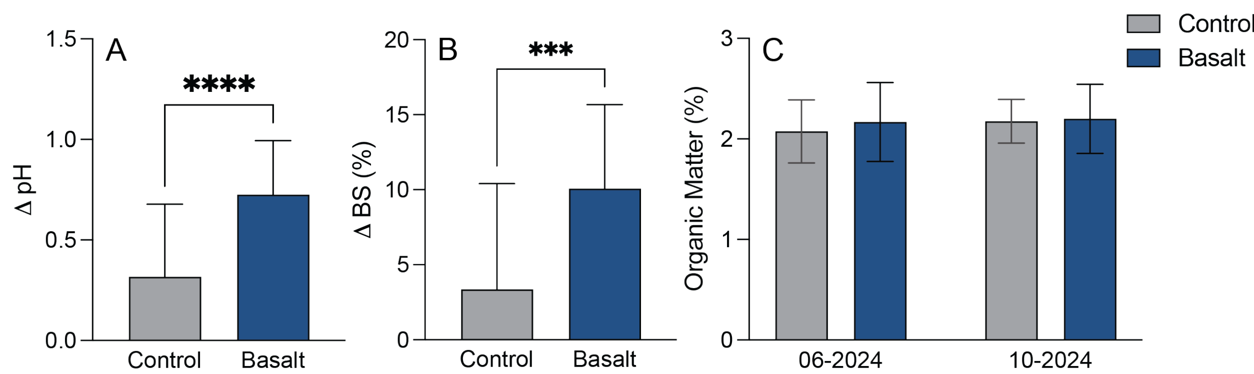

Figure 1. Agronomic soil properties prior to and following the growing season for control plots (gray) and basalt-amended plots (blue). A, B) Relative changes in soil pH and base saturation (BS %) of the post-harvest samples relative to pre-planting. C) The total organic matter (%) of the control and basalt-amended plots for each sampling month is shown. Bars represent mean ± one standard error.

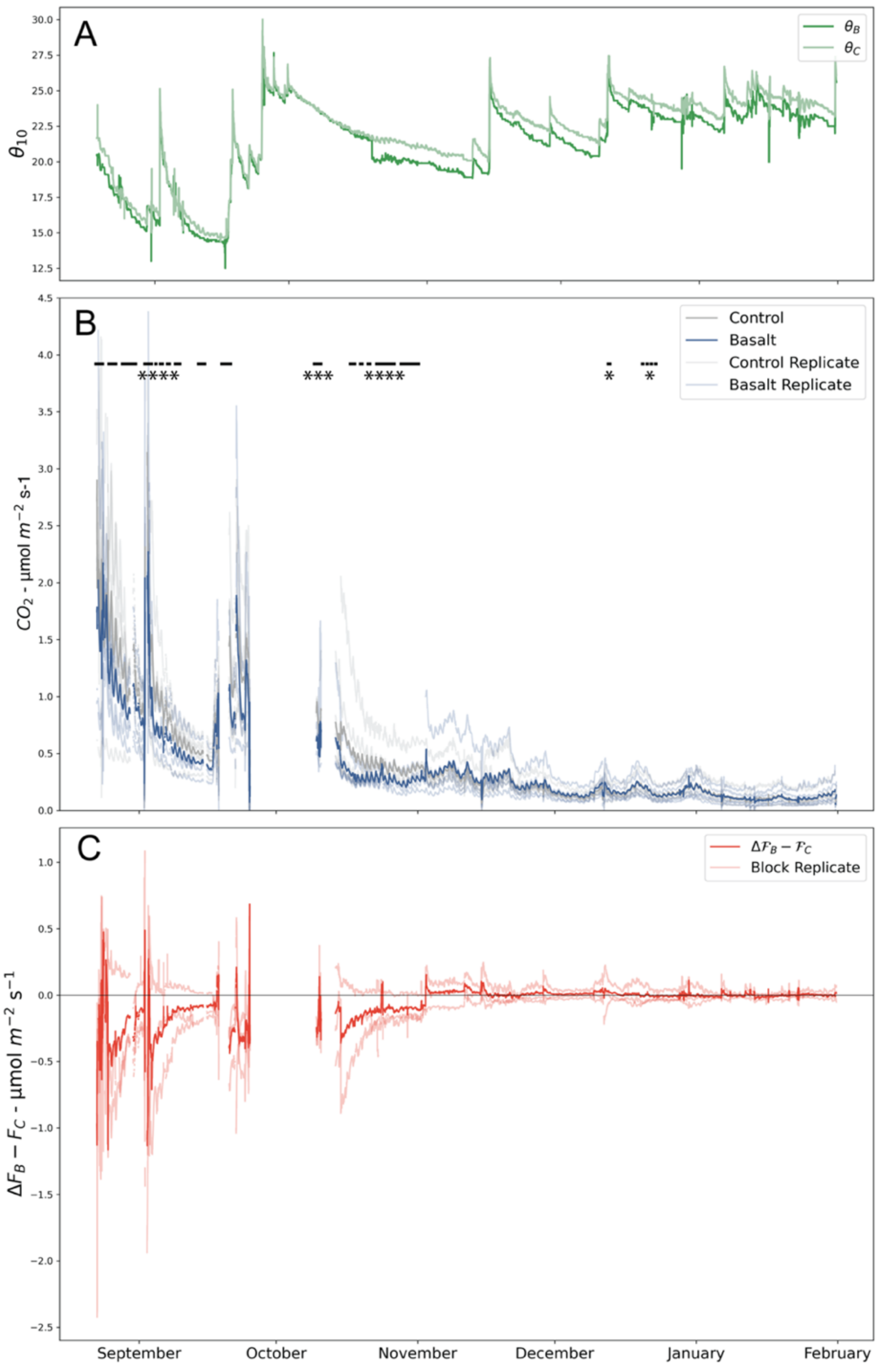

Figure 2: Comparisons of volumetric water content % (θ), CO_2 flux (μmol m^{-2} s^{-1}), and difference between basalt flux (F_B) and control flux (F_C) (μmol m^{-2} s^{-1}) for control and basalt-amended plots over the measurement period. A) θ over time is represented as an average of monitored control (light green) and basalt (dark green) plots, respectively, with error being ≤ 1% B) The CO_2 flux (μmol m^{-2} s^{-1}) over time shows overall averages for control (gray) and basalt (blue) in bold, with individual replicate values for each plot shown. C) ΔF_B-F_C over time shows overall average subtraction in bold, with individual replicate subtractions for blocks also shown. ****$p<0.001$, ***$p<0.005$, *$p<0.05$.

This can largely be attributed to the active crop growth during this period, leading to high respiration rates from root matter, and continuous additions in organic compounds leading to higher CO_2 production by microbes in soils[28–31]. There are also clear prominent pulses aligning with θ, indicating the clear relationship between weathering and water availability within soils[32,33]. $F_{0\text{-}10}$ pulses, attributed to freeze-thaw cycling, were seen for both basalt and control within the winter months, but no differences were seen with treatment. Periods of exceptionally high weathering demonstrate the roles that both water availability, season, and crop activity play in regulating weathering rates within agricultural systems. Differences in these site-specific factors likely lead to divergence in weathering rates between current field trial deployments as well as highly engineered mesocosm studies.

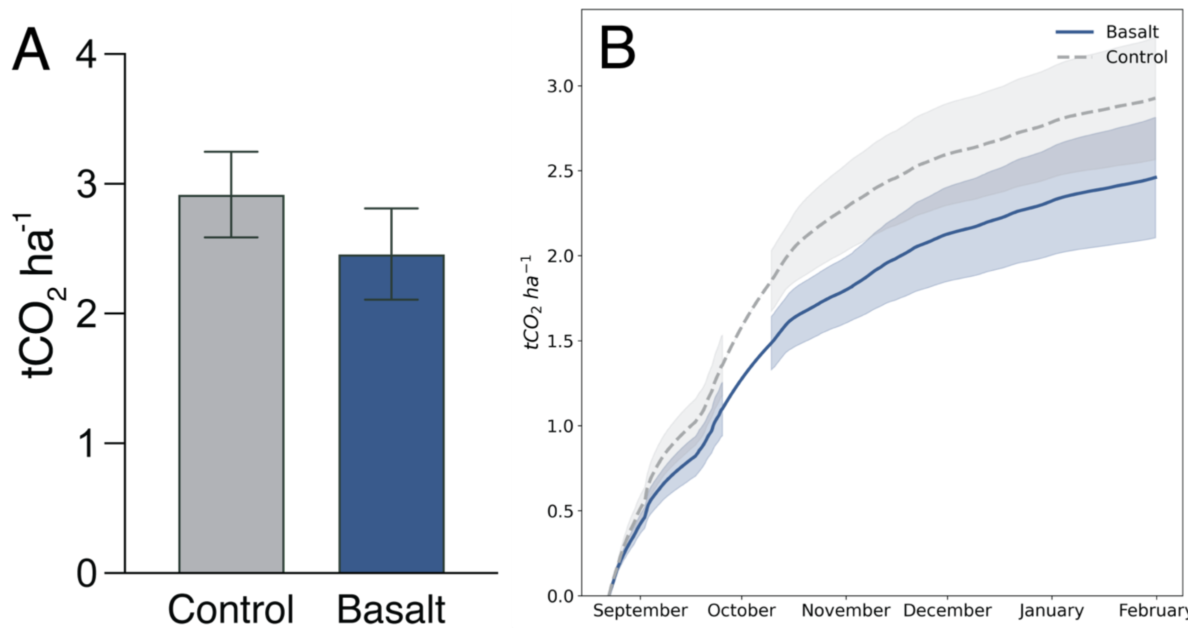

Figure 3. Cumulative emissive flux of CO_2 (tCO_2 ha^{-1}) over a half-year monitoring timeframe for control (grey) and basalt (blue) amended plots. A) The total average cummulative flux at the end of January with bars representing mean ± one standard error. B) The average cummulative change over time is shown in bold, with control and basalt SEM for the measurement period respectively shaded.

At the beginning of February 2025, the cumulative control flux was 2.92 ± 0.33 t ha^{-1}, and the cumulative basalt flux totaled to 2.46 ± 0.35 t ha^{-1} (Fig. 3a). In total, there is a cumulative decrease of 0.46 ± 0.5 t ha^{-1} equating to a conservative immediate weathering rate of 1.04 t $ha^{-1}yr^{-1}$. This estimate is lower than previous estimates of weathering rates in North American field studies using basalt, but should be considered a minimum estimate given that most cations on a short time scale are predicted to move onto sorption sites[10,20,34]. The observed shift in base saturation indicates that at least half of the cations released during weathering are moved onto sorption sites in the uppermost portion of the soil column. This process releases acid into soil waters, temporarily reversing the CO_2 uptake[18,35]. Despite this reversal, the persistent decrease in $F_{0\text{-}10}$ demonstrates that there is still cation transport through these exchange sites.

This CO_2 flux-based CDR estimate highlights the importance of CO_2 originating from soil respiration, as opposed to from rainwater directly. This aligns with previous studies demonstrating that mineral dissolution occurs rapidly in CO_2-rich environments as opposed to atmospheric concentrations[36]. The loss of weathering following growing season, however, demonstrates that soil organic matter respiration and precipitation in cool weathering conditions are not enough to lead to appreciable weathering rates (Fig. 3b).

The clear fluctuation in weathering rate, even within a month time scale, also demonstrates the importance of continuous monitoring, as opposed to instantaneous measurements, in understanding gas-phase signals. This work calls into question if sporadic soil water or gas phase measurements can be used to properly track carbon fluxes. However, this work supports that embedded soil CO_2 sensors can give robust minimum estimates of weathering rates and provide an additional line of evidence for significant rapid weathering with basalt addition to croplands.

Acknowledgements

We thank Tim Jesper Surhoff for his advice in modelling loss periods, as well as the advice of Eric Slessarev on flux analysis. We acknowledge Farmblox for their custom continuous-logging sensor design. NJP acknowledges support from Microsoft and the Yale Center for Natural Carbon Capture.

Conflict of Interest

NJP was a co-founder of the carbon dioxide removal company Lithos Carbon but has no financial ties to the company.

Supporting Information

Figure 1. Full soil profile of experimental region. Soil horizons are demarcated at each horizon boundary. Beyond 1m, the soil moved to saprolite.

References

(1) *Emissions Gap Report 2024 | UNEP - UN Environment Programme.* https://www.unep.org/resources/emissions-gap-report-2024 (accessed 2025-03-10).

(2) Smith, S.; Geden, O.; Gidden, M. J.; Lamb, W. F.; Nemet, G. F.; Minx, J. C.; Buck, H.; Burke, J.; Cox, E.; Edwards, M. R.; Fuss, S.; Johnstone, I.; Müller-Hansen, F.; Pongratz, J.; Probst, B. S.; Roe, S.; Schenuit, F.; Schulte, I.; Vaughan, N. E. The State of Carbon Dioxide Removal 2024 - 2nd Edition., 2024. DOI 10.17605/OSF.IO/F85QJ.

(3) Buylova, A.; Fridahl, M.; Nasiritousi, N.; Reischl, G. Cancel (Out) Emissions? The Envisaged Role of Carbon Dioxide Removal Technologies in Long-Term National Climate Strategies. *Front. Clim.* **2021**, *3*. https://doi.org/10.3389/fclim.2021.675499.

(4) Securing Our Future: Europe's 2040 Climate Target and Path to Climate Neutrality by 2050 Building a Sustainable, Just and Prosperous Society. https://eur-lex.europa.eu/legal-content/EN/TXT/?uri=COM%3A2024%3A63%3AFIN (2024).

(5) Scott, V.; Haszeldine, R. S.; Tett, S. F. B.; Oschlies, A. Fossil Fuels in a Trillion Tonne World. *Nature Clim Change* **2015**, *5* (5), 419–423. https://doi.org/10.1038/nclimate2578.

(6) Allen, M. R.; Friedlingstein, P.; Girardin, C. A. J.; Jenkins, S.; Malhi, Y.; Mitchell-Larson, E.; Peters, G. P.; Rajamani, L. Net Zero: Science, Origins, and

Implications. *Annual Review of Environment and Resources* **2022**, *47* (Volume 47, 2022), 849–887. https://doi.org/10.1146/annurev-environ-112320-105050.

(7) Dooley, K.; Keith, H.; Larson, A.; Ctacora-Vargas, G.; Carton, W.; Christinsen, K. L. The Land Gap Report 2022. https://landgap.org/2022/report (2022).

(8) Beerling, D. J.; Kantzas, E. P.; Lomas, M. R.; Taylor, L. L.; Zhang, S.; Kanzaki, Y.; Eufrasio, R. M.; Renforth, P.; Mecure, J.-F.; Pollitt, H.; Holden, P. B.; Edwards, N. R.; Koh, L.; Epihov, D. Z.; Wolf, A.; Hansen, J. E.; Banwart, S. A.; Pidgeon, N. F.; Reinhard, C. T.; Planavsky, N. J.; Val Martin, M. Transforming US Agriculture for Carbon Removal with Enhanced Weathering. *Nature* **2025**, 1–10. https://doi.org/10.1038/s41586-024-08429-2.

(9) Hartmann, J.; West, A. J.; Renforth, P.; Köhler, P.; De La Rocha, C. L.; Wolf-Gladrow, D. A.; Dürr, H. H.; Scheffran, J. Enhanced Chemical Weathering as a Geoengineering Strategy to Reduce Atmospheric Carbon Dioxide, Supply Nutrients, and Mitigate Ocean Acidification. *Reviews of Geophysics* **2013**, *51* (2), 113–149. https://doi.org/10.1002/rog.20004.

(10) Beerling, D. J.; Epihov, D. Z.; Kantola, I. B.; Masters, M. D.; Reershemius, T.; Planavsky, N. J.; Reinhard, C. T.; Jordan, J. S.; Thorne, S. J.; Weber, J.; Val Martin, M.; Freckleton, R. P.; Hartley, S. E.; James, R. H.; Pearce, C. R.; DeLucia, E. H.; Banwart, S. A. Enhanced Weathering in the US Corn Belt Delivers Carbon Removal with Agronomic Benefits. *Proc Natl Acad Sci U S A* **2024**, *121* (9), e2319436121. https://doi.org/10.1073/pnas.2319436121.

(11) Beerling, D. J.; Leake, J. R.; Long, S. P.; Scholes, J. D.; Ton, J.; Nelson, P. N.; Bird, M.; Kantzas, E.; Taylor, L. L.; Sarkar, B.; Kelland, M.; DeLucia, E.; Kantola, I.; Müller, C.; Rau, G.; Hansen, J. Farming with Crops and Rocks to Address Global Climate, Food and Soil Security. *Nature Plants* **2018**, *4* (3), 138–147. https://doi.org/10.1038/s41477-018-0108-y.

(12) Dietzen, C.; Harrison, R.; Michelsen-Correa, S. Effectiveness of Enhanced Mineral Weathering as a Carbon Sequestration Tool and Alternative to Agricultural Lime: An Incubation Experiment. *International Journal of Greenhouse Gas Control* **2018**, *74*, 251–258. https://doi.org/10.1016/j.ijggc.2018.05.007.

(13) Costa, D.; Sutter, C.; Shepherd, A.; Jarvie, H.; Wilson, H.; Elliott, J.; Liu, J.; Macrae, M. Impact of Climate Change on Catchment Nutrient Dynamics: Insights from around the World. *Environ. Rev.* **2023**, *31* (1), 4–25. https://doi.org/10.1139/er-2021-0109.

(14) Clarkson, M. O.; Larkin, C. S.; Swoboda, P.; Reershemius, T.; Suhrhoff, T. J.; Maesano, C. N.; Campbell, J. S. A Review of Measurement for Quantification of Carbon Dioxide Removal by Enhanced Weathering in Soil. *Front. Clim.* **2024**, *6*. https://doi.org/10.3389/fclim.2024.1345224.

(15) Almaraz, M.; Bingham, N. L.; Holzer, I. O.; Geoghegan, E. K.; Goertzen, H.; Sohng, J.; Houlton, B. Z. Methods for Determining the CO2 Removal Capacity of

Enhanced Weathering in Agronomic Settings. *Front. Clim.* **2022**, *4*. https://doi.org/10.3389/fclim.2022.970429.

(16) Suhrhoff, T. J.; Reershemius, T.; Wang, J.; Jordan, J. S.; Reinhard, C. T.; Planavsky, N. J. A Tool for Assessing the Sensitivity of Soil-Based Approaches for Quantifying Enhanced Weathering: A US Case Study. *Front. Clim.* **2024**, *6*. https://doi.org/10.3389/fclim.2024.1346117.

(17) Larkin, C. S.; Andrews, M. G.; Pearce, C. R.; Yeong, K. L.; Beerling, D. J.; Bellamy, J.; Benedick, S.; Freckleton, R. P.; Goring-Harford, H.; Sadekar, S.; James, R. H. Quantification of CO2 Removal in a Large-Scale Enhanced Weathering Field Trial on an Oil Palm Plantation in Sabah, Malaysia. *Front. Clim.* **2022**, *4*. https://doi.org/10.3389/fclim.2022.959229.

(18) Kanzaki, Y.; Planavsky, N.; Zhang, S.; Jordan, J.; Suhrhoff, T. J.; Reinhard, C. T. Soil Cation Storage as a Key Control on the Timescales of Carbon Dioxide Removal through Enhanced Weathering.

(19) Dietzen, C.; Rosing, M. T. Quantification of CO2 Uptake by Enhanced Weathering of Silicate Minerals Applied to Acidic Soils. *International Journal of Greenhouse Gas Control* **2023**, *125*, 103872. https://doi.org/10.1016/j.ijggc.2023.103872.

(20) Kantola, I. B.; Blanc-Betes, E.; Masters, M. D.; Chang, E.; Marklein, A.; Moore, C. E.; von Haden, A.; Bernacchi, C. J.; Wolf, A.; Epihov, D. Z.; Beerling, D. J.; DeLucia, E. H. Improved Net Carbon Budgets in the US Midwest through Direct Measured Impacts of Enhanced Weathering. *Global Change Biology* **2023**, *29* (24), 7012–7028. https://doi.org/10.1111/gcb.16903.

(21) Stubbs, A. R.; Paulo, C.; Power, I. M.; Wang, B.; Zeyen, N.; Wilson, S. Direct Measurement of CO2 Drawdown in Mine Wastes and Rock Powders: Implications for Enhanced Rock Weathering. *International Journal of Greenhouse Gas Control* **2022**, *113*, 103554. https://doi.org/10.1016/j.ijggc.2021.103554.

(22) Chiaravalloti, I.; Theunissen, N.; Zhang, S.; Wang, J.; Sun, F.; Ahmed, A. A.; Pihlap, E.; Reinhard, C. T.; Planavsky, N. J. Mitigation of Soil Nitrous Oxide Emissions during Maize Production with Basalt Amendments. *Front. Clim.* **2023**, *5*. https://doi.org/10.3389/fclim.2023.1203043.

(23) Vargas, R.; Detto, M.; Baldocchi, D. D.; Allen, M. F. Multiscale Analysis of Temporal Variability of Soil CO2 Production as Influenced by Weather and Vegetation. *Global Change Biology* **2010**, *16* (5), 1589–1605. https://doi.org/10.1111/j.1365-2486.2009.02111.x.

(24) Maier, M.; Schack-Kirchner, H. Using the Gradient Method to Determine Soil Gas Flux: A Review. *Agricultural and Forest Meteorology* **2014**, *192–193*, 78–95. https://doi.org/10.1016/j.agrformet.2014.03.006.

(25) Oerter, E.; Mills, J. V.; Maurer, G. E.; Lammers, L. N.; Amundson, R. Greenhouse Gas Production and Transport in Desert Soils of the Southwestern United States. *Global Biogeochemical Cycles* **2018**, *32* (11), 1703–1717. https://doi.org/10.1029/2018GB006035.

(26) Massman, W. J. A Review of the Molecular Diffusivities of H2O, CO2, CH4, CO, O3, SO2, NH3, N2O, NO, and NO2 in Air, O2 and N2 near STP. *Atmospheric Environment* **1998**, *32* (6), 1111–1127. https://doi.org/10.1016/S1352-2310(97)00391-9.
(27) Moldrup, P.; Olesen, T.; Yamaguchi, T.; Schjønning, P.; Rolston, D. E. Modeling diffusion and reaction in soils: IX. The Buckingham-Burdine-Campbell equation for gas diffusivity in undisturbed soil. *Soil Science* **1999**, *164* (8), 542.
(28) Deng, H.; Sonnenthal, E.; Arora, B.; Breunig, H.; Brodie, E.; Kleber, M.; Spycher, N.; Nico, P. The Environmental Controls on Efficiency of Enhanced Rock Weathering in Soils. *Sci Rep* **2023**, *13* (1), 9765. https://doi.org/10.1038/s41598-023-36113-4.
(29) Buss, W.; Hasemer, H.; Sokol, N. W.; Rohling, E. J.; Borevitz, J. Applying Minerals to Soil to Draw down Atmospheric Carbon Dioxide through Synergistic Organic and Inorganic Pathways. *Commun Earth Environ* **2024**, *5* (1), 1–11. https://doi.org/10.1038/s43247-024-01771-3.
(30) Balland-Bolou-Bi, C.; Poszwa, A. Effect of Calco-Magnesian Amendment on the Mineral Weathering Abilities of Bacterial Communities in Acidic and Silicate-Rich Soils. *Soil Biology and Biochemistry* **2012**, *50*, 108–117. https://doi.org/10.1016/j.soilbio.2012.02.034.
(31) Verbruggen, E.; Struyf, E.; Vicca, S. Can Arbuscular Mycorrhizal Fungi Speed up Carbon Sequestration by Enhanced Weathering? *PLANTS, PEOPLE, PLANET* **2021**, *3* (5), 445–453. https://doi.org/10.1002/ppp3.10179.
(32) Cipolla, G.; Calabrese, S.; Porporato, A.; Noto, L. V. Effects of Precipitation Seasonality, Irrigation, Vegetation Cycle and Soil Type on Enhanced Weathering – Modeling of Cropland Case Studies across Four Sites. *Biogeosciences* **2022**, *19* (16), 3877–3896. https://doi.org/10.5194/bg-19-3877-2022.
(33) Calabrese, S.; Wild, B.; Bertagni, M. B.; Bourg, I. C.; White, C.; Aburto, F.; Cipolla, G.; Noto, L. V.; Porporato, A. Nano- to Global-Scale Uncertainties in Terrestrial Enhanced Weathering. *Environ. Sci. Technol.* **2022**, *56* (22), 15261–15272. https://doi.org/10.1021/acs.est.2c03163.
(34) Lewis, A. L.; Sarkar, B.; Wade, P.; Kemp, S. J.; Hodson, M. E.; Taylor, L. L.; Yeong, K. L.; Davies, K.; Nelson, P. N.; Bird, M. I.; Kantola, I. B.; Masters, M. D.; DeLucia, E.; Leake, J. R.; Banwart, S. A.; Beerling, D. J. Effects of Mineralogy, Chemistry and Physical Properties of Basalts on Carbon Capture Potential and Plant-Nutrient Element Release via Enhanced Weathering. *Applied Geochemistry* **2021**, *132*, 105023. https://doi.org/10.1016/j.apgeochem.2021.105023.
(35) te Pas, E. E. E. M.; Chang, E.; Marklein, A. R.; Comans, R. N. J.; Hagens, M. Accounting for Retarded Weathering Products in Comparing Methods for Quantifying Carbon Dioxide Removal in a Short-Term Enhanced Weathering Study. *Front. Clim.* **2025**, *6*. https://doi.org/10.3389/fclim.2024.1524998.

(36) Amann, T.; Hartmann, J.; Hellmann, R.; Pedrosa, E. T.; Malik, A. Enhanced Weathering Potentials—the Role of in Situ CO2 and Grain Size Distribution. *Front. Clim.* **2022**, *4*. https://doi.org/10.3389/fclim.2022.929268.